Luzi, M., Girod, M., Naumann, R., Schicks, J. M., Erzinger, J. (2010): A high pressure cell for kinetic studies on gas hydrates by powder X-ray diffraction. - Review of Scientific Instruments, 81, 125105

DOI: 10.1063/1.3520465

A high-pressure cell for kinetic studies on gas hydrates by powder X-ray diffraction

Manja Luzi,[a] Matthias Girod,[b] Rudolf Naumann, Judith M. Schicks, and Jörg Erzinger
Helmholtz-Centre Potsdam, German Research Centre for Geosciences (GFZ), Telegrafenberg, D-14473 Potsdam, Germany

(Received 14 September 2010; accepted 5 November 2010; published online XX XX XXXX)

A new high-pressure–low-temperature cell was developed for *in situ* observations of gas hydrates by powder X-ray diffraction. The experimental setup allows investigating hydrate formation and dissociation as well as transformation processes between different hydrate crystal structures as a function of pressure, temperature, and feed gas composition. Due to a continuous gas flow, the composition of the gas phase is kept constant during the whole experiment. This is crucial for the formation of mixed hydrates formed from feed gas mixtures that contain one or more components in low concentrations. The pressure cell can be used in a pressure range between 0.1 and 4.0 MPa and a temperature range between 248 and 298 K. First results of time-resolved measurements of a mixed structure II CH_4 + iso-C_4H_{10} hydrate and a structure I CO_2 hydrate are presented. © *2010 American Institute of Physics*. [doi:10.1063/1.3520465]

I. INTRODUCTION

Gas hydrates are crystalline ice-like solids that consist of a three-dimensional network of water molecules. The water molecules are connected via hydrogen bonds forming cavities. The water cavities are stabilized by small guest molecules, usually in the range between 0.3 and 0.8 nm. Depending on the size of the guest molecule, different hydrate crystal structures form. Naturally occurring gas hydrates predominantly include not only CH_4 but also C_2–C_5 hydrocarbons, CO_2, and H_2S, which results in three commonly known crystal structures: the cubic structures I and II and the hexagonal structure H. Gas hydrates form from liquid water or ice and in presence of sufficient amounts of gas under elevated pressures and at low temperatures. These conditions are given in permafrost regions and at the seafloor as well as in gas and oil pipelines.[1,2] But the mechanisms of the formation of natural gas hydrates have not been finally clarified yet. Due to the high risk of potential hydrate plugs in pipelines, the formation and growth of gas hydrates should be avoided. The understanding of hydrate formation and growth processes and its kinetics is of fundamental relevance for the prevention of hydrate plugs in pipelines and the understanding of natural processes.

In the past, some kinetic studies on gas hydrate formation and growth processes as well as dissociation processes were performed employing a wide range of techniques such as neutron and X-ray diffraction (XRD), NMR, and Raman spectroscopy. *In situ* neutron and XRD experiments are valuable tools to identify crystalline phases and to obtain qualitative and quantitative information about crystal structural changes during hydrate formation and dissociation. Time-resolved results from *in situ* neutron diffraction measurements on gas hydrates formed from CH_4 or CO_2 and grained ice were published among others by Henning *et al.*,[3] Wang *et al.*,[4] Staykova *et al.*,[5] and Genov *et al.*[6] The pressures applied varied between 0.1 and 6.9 MPa. The feed gas phase consisted of only one component. Although neutron diffraction is a powerful tool to follow structural changes that occur during the transformation of ice into hydrate, the technical and financial efforts are very demanding. Results from time-dependent energy-dispersive synchrotron XRD studies were presented for instance by Koh *et al.*[7] and Tang *et al.*[8] They studied the crystallization process of CO_2 and C_3H_8 hydrate at 3.29 and 0.42 MPa, respectively. Another energy-dispersive XRD method was used by Takeya *et al.*[9] to investigate the formation process of CO_2 hydrate at 0.98 MPa. In 2003, Takeya *et al.*[10] presented results for a mixed CH_4 + C_2H_6 hydrate formation from hexagonal ice by means of *in situ* time-resolved energy-dispersive XRD. As the composition of the gas phase changed during hydrate formation, they determined the initial and final composition of the gas phase by gas chromatography. Various studies focus on the dissociation process of gas hydrates with a particular emphasis on a possible self-preservation effect. By use of time-resolved powder XRD, Takeya *et al.*[11] recently analyzed the self-preservation effect of CH_4 hydrate at ambient pressure and defined temperatures. They also investigated the dissociation behavior of gas hydrates with respect to the trapped guest molecules by means of temperature-dependent powder XRD.[12]

Most of the above mentioned diffraction experiments have in common that the gas phase consists of only one component. But natural gas hydrates can also show complex compositions as it was presented for hydrate samples recovered from the Cascadia margin or the Gulf of Mexico by Lu *et al.*[13] and Sassen *et al.*,[14] respectively. Laboratory *in situ* investigations on gas hydrate formation from feed gas mixtures are generally difficult because the composition of the gas phase may change over time in case of a limited gas reservoir. Especially in case of components with low concentrations in the

[a]Electronic mail: mluzi@gfz-potsdam.de
[b]Present address: BAM Federal Institute for Materials Research and Testing, Richard-Willstätter-Straße 11, D-12489 Berlin, Germany.

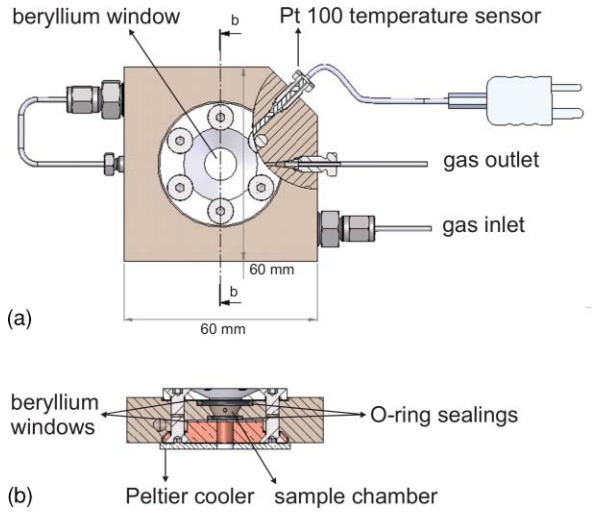

FIG. 1. (Color online) Sketch of the pressure cell from (a) top view and (b) side view.

feed gas or the enrichment of these components in the hydrate phase, the depletion of these components in the gas phase is very likely. To provide an almost constant composition of the gas phase during the formation of mixed gas hydrates, either the volume of the gas phase has to be huge enough or the gas phase has to be refreshed by using a continuous gas flow. In this study, we present a new cell design that considers this aspect and ensures a constant composition of the feed gas phase. Compared to neutron or synchrotron XRD, the experimental setup presented here is less demanding; nevertheless, it enables fast and precise measurements.

II. EXPERIMENTAL SETUP

A. Cell design

The body of the newly designed sample cell is made of stainless steel with a hole of 0.5 cm diameter in its center. The cell volume is approximately 250 μl. Both sides of the cell body are sealed with beryllium plates and tightened with O-rings. Beryllium was chosen as window material due to its excellent X-ray transparency in combination with high-pressure stability. The beryllium plates have a thickness of 1.5 mm and are therefore pressure resistant up to 4 MPa. Due to the opposing beryllium windows, the cell can be transmitted by the X-rays in order to obtain the powder XRD pattern. Figure 1 presents a sketch of the pressure cell in top view (a) and side view (b).

The temperature is controlled by means of a Peltier cooling device from Kryotherm type TB-119-1.4-1.15CH that also contains a hole of 0.5 cm. The Peltier cooling device provides quick temperature changes and a precise temperature control of $\pm$1.0 K by use of an adjustable power source and a controlling device (West 4200, West Instruments Ltd.). The cell can be operated in a temperature range between 253 and 288 K. The temperature is determined by use of a calibrated Pt 100 temperature sensor. The temperature sensor is located within 1 mm to the sample chamber.

The sample cell is pressurized with the hydrate forming gas from a gas cylinder to a defined pressure above the equilibrium pressure at given temperature. The pressure is regulated with an ER 3000 pressure regulator (Tescom Corp.) with a precision of 2% (rel.). The applicable pressure ranges between 0.1 and 4.0 MPa. Furthermore, the experimental setup is run with a continuous gas flow. Therefore, the pressure and the composition of the gas phase can be kept constant during the experiment. The gas flow rate is adjusted to 1 ml/min. During the experiment, the gas flow is measured and controlled with a commercial flowmeter F-230M-AAA-11-Z from Bronkhorst. The flowmeter is situated behind the pressure cell and regulates the gas flow to 1 ml/min automatically. The supply pipes for the incoming and the outgoing gas are labeled in the schematic overview of the sample cell in Fig. 1. The incoming gas is directed through the cooled cell body in order to precool the feed gas before it enters the sample chamber. Due to constructional reasons, it leaves the cell body again and is redirected to the sample chamber. This part of the tubing is isolated against ambient temperature, which is not shown in Fig. 1. Pressure and gas flow are recorded during the experiment.

The cell body is embedded into a casing of polyoxymethylene (Delrin^{TM}), which enables a thermal isolation against the ambient temperature. Furthermore, the frame serves as mounting element on the sample table of the diffractometer. Figure 2 presents a photograph of the pressure cell mounted on the XYZ stage of the diffractometer. It shows the sample cell while running in transmission mode.

B. Diffractometer

The cell was designed for the use in combination with a Bruker AXS D8 Discover microdiffractometer with Cu-K_α radiation generated at 40 kV and 40 mA. The diffractometer has parallel beam optics (Goebel mirror) to optimize the beam intensity, which enables the analysis of powder samples with a nonplanar surface. Additionally, a monocapillary, which narrows the beam to a diameter of 300 μm, was applied. In consequence, small sample areas and consequently small sample amounts of gas hydrate powder can be investigated in the micrometer range. The detection of the diffracted X-rays is carried out with GADDS (General Area Detection Diffraction System), which includes a HI-STAR area detector. Within 1 min, the diffraction lines between 5° and 37° 2θ can be collected simultaneously in a single frame of the detector. The GADDS image (frame) shows sectors from the cones of diffraction with a radius of 2θ that result from the diffraction of the X-rays on each lattice plane hkl. Microcrystalline samples form smooth diffraction rings (Debye–Scherrer rings). Single crystals show diffraction spots that lie along the ring of 2θ. By use of the GADDS software, the intensity of the rings within the sector is integrated. This results in a conventional diffractogram (2θ angle versus intensity).[15] The 2θ versus intensity plots can be imported as raw files into diverse analysis software. Figure 3 presents a GADDS image of a structure II CH_4 + iso-C_4H_{10} hydrate with the respective 2θ versus intensity plot (powder XRD pattern).

C. Experimental procedure

For a typical experiment, finely powdered ice is prepared at first. The ice is generated from ca. 3 ml deionized water

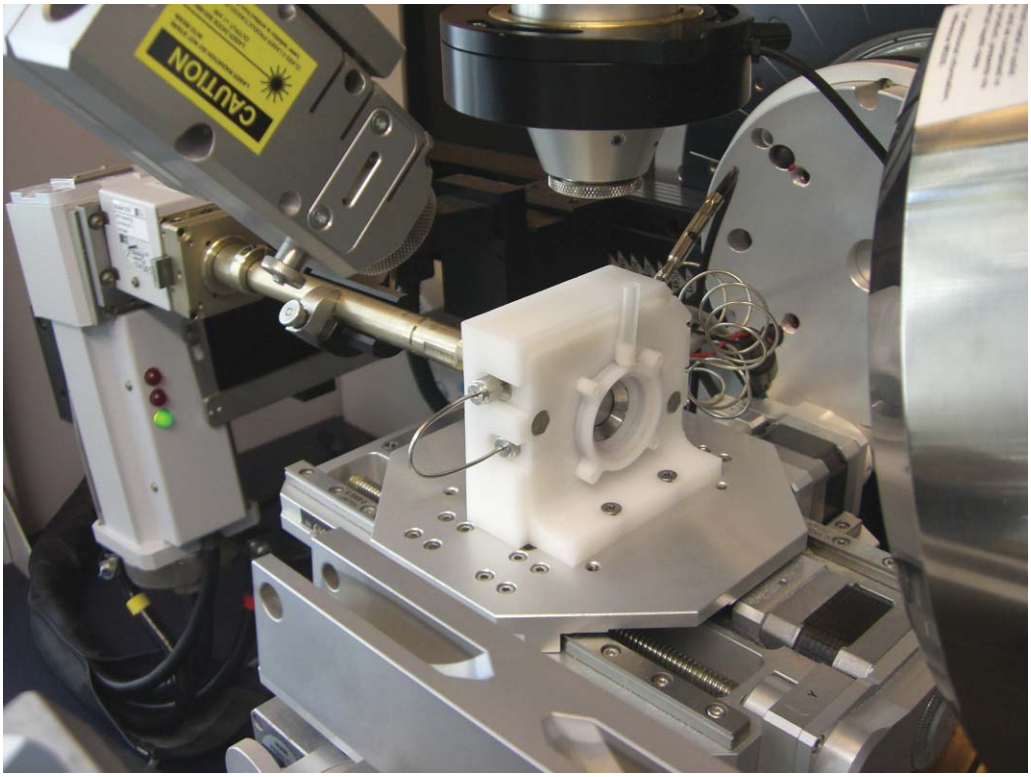

FIG. 2. (Color online) Photograph of the pressure cell mounted on the XYZ stage of the diffractometer.

that is frozen in a liquid nitrogen bath. Afterward, the ice is powdered in a 6750 freezer mill (Spex CertiPrep) that is also cooled with liquid nitrogen. By means of scanning electron microscopy, the diameter of these ice particles was accounted to be less than 10 μm. At next, the precooled sample cell is filled with approximately 150 μl powdered ice, carefully sealed, and mounted on the XYZ stage of the diffractometer. Thereby, the ice sticks on the beryllium window, which is situated on the side of the Peltier cooling device. In the next step, the sample cell is pressurized with the respective gas or gas mixture, and the data acquisition is commenced. The frequency of data collection depends on the transformation rate of ice into hydrate. Due to the narrow beam, various positions within the sample can be measured in a short sequence. Commonly, five defined measuring points, which are randomly distributed within the sample cell, are chosen for analysis. Accordingly, more detailed information about the sample composition regarding possible inhomogeneities can be obtained. Figure 4 presents the transformation of hexagonal ice into a cubic structure II hydrate, which was formed from a gas mixture of 98% CH_4 and 2% iso-C_4H_{12}. The hydrate was grown at 1.06 MPa and 267 K. The transformation process is shown for one measuring point. In order to distinguish between the ice and the hydrate phase, the diffraction peaks are labeled by the Miller indices of the respective crystal planes. At the beginning of the experiment, only the four ice reflections occur (see Fig. 4 at $t = 0$). Within 10 min, the start of the hydrate crystal formation accompanies with the occurrence of the hydrate reflections. In the course of the experiment, the hydrate reflections increase while the ice reflection intensities decrease. This leads to the conclusion that the ice phase is converted into a structure II gas hydrate. Figure 3 shows the powder XRD pattern at the time the ice is completely converted into the structure II CH_4 + iso-C_4H_{10} hydrate.

At least, three types of experiments can be performed using this experimental setup. Next to the experiments concerning gas hydrate formation rates that were described above also hydrate dissociation rates can be determined. In this case, a pure hydrate phase has to be synthesized at first. Afterward, hydrate dissociation can be induced by pressure release or increase of temperature. It has to be considered that experiments regarding hydrate formation and dissociation rates have to be done below 273 K to retain the ice phase. Otherwise the water/hydrate crystal mixture would slip off the beryllium window because the sample cell is run in a vertical position in transmission mode (see Fig. 2). The third type of experiments includes the analysis of phase transformations between different hydrate crystal structures that can be caused by pressure or temperature changes. Due to the continuous gas flow, it can be assured that these phase transformations do not result from the depletion of one guest species in the gas phase. But the experimental setup also provides the opportunity to change the gas supply. Thus, transformations of the hydrate crystal structure can be observed that are induced by a change of the offered guest molecules.

III. DATA ANALYSIS AND FIRST RESULTS

As it is described by Wölfel,[16] the integrated intensity I of a reflex is proportional to the crystal volume V. A change of the integrated intensity is therefore associated with a

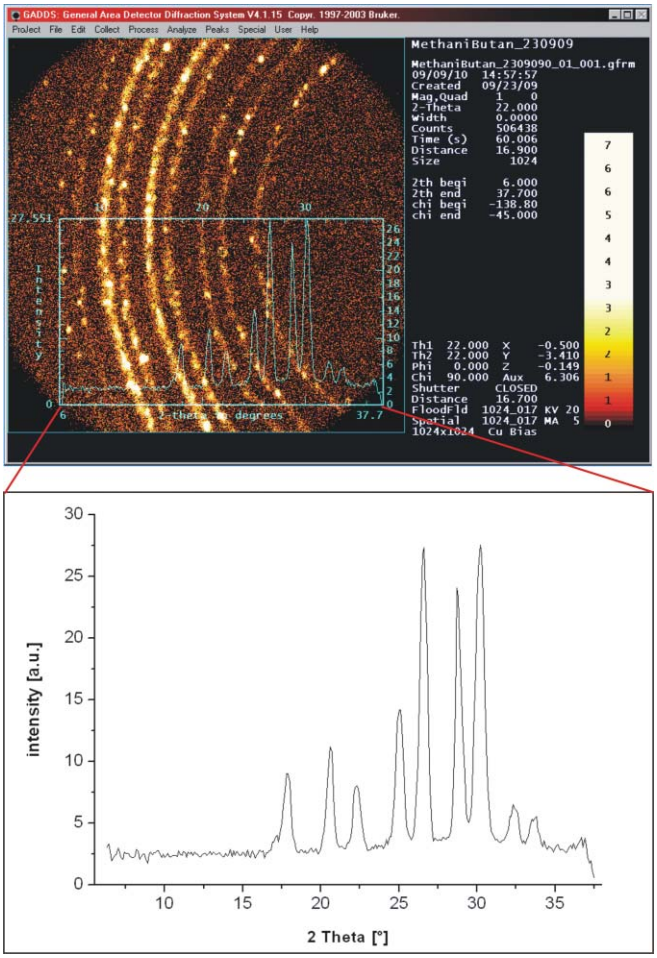

FIG. 3. (Color online) GADDS image with 2θ versus intensity plot of a structure II CH_4 + iso-C_4H_{10} gas hydrate.

volume change of the hydrate or ice phase. The rate of change provides information about formation, dissociation, or transformation rates of the hydrate crystals.[9] In order to estimate the progress of such a process, a representative reflection of the respective phase has to be chosen. At next, the integrated intensity of this diffraction peak from the pure phase is determined. The calculation of the peak areas is done by means of the Bruker AXS TOPAS program. The intensity ratio I/I_0, where I_0 is the integrated intensity of the pure phase, can be given for the respective phase as a function of time. As we obtain data from five measuring points, a mean value for the intensity ratio can be determined. The error is given by the standard deviation.

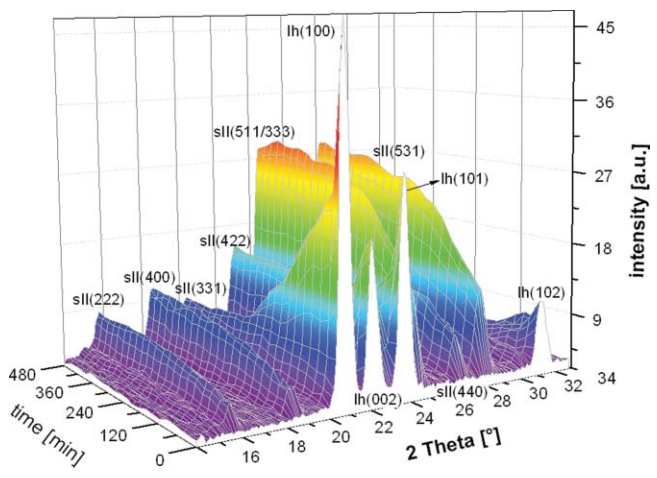

FIG. 4. (Color online) Powder X-ray diffractograms as a function of time collected during CH_4 + iso-C_4H_{10} hydrate formation from ice at one measuring point at 267 K and 1.06 MPa.

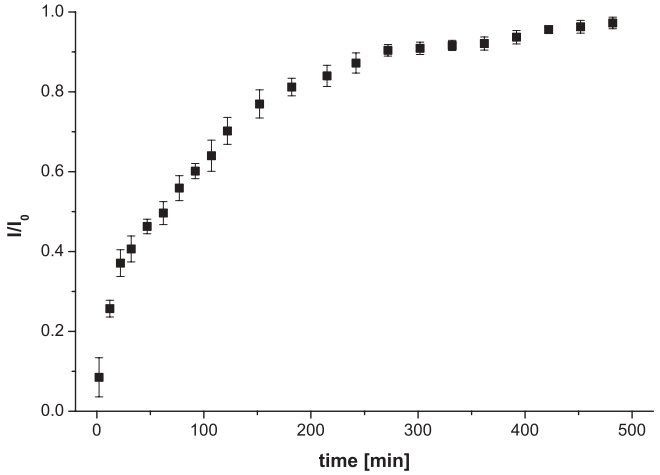

FIG. 5. Mean intensity ratio I/I_0 as a function of time during CH_4 + iso-C_4H_{10} hydrate formation from ice at 267 K and 1.06 MPa.

Figure 5 shows the relative intensity ratio I/I_0 of growing CH_4 + iso-C_4H_{10} hydrates as a function of time. This experiment was started from a pure ice phase like it is described above. The system was pressurized to 1.06 MPa and run at 267 K until the ice phase was completely converted into hydrate. While Fig. 4 presents the formation process for one measuring point of this experiment, Fig. 5 shows the mean formation rate for all data points. The small error bars refer to a homogenous formation of the hydrate phase. The reflection for the sII (531) crystal plane at approximately 30.5° 2θ was used to calculate the intensity ratio and to estimate the formation rate of the double hydrate. This reflection was chosen because it does not overlap with reflections from the ice phase. It becomes obvious from Fig. 5 that 8 h are sufficient for an almost complete conversion of ice Ih into structure II CH_4 + iso-C_4H_{10} hydrate.

The reproducibility of the data obtained from this experimental setup is shown by the following example. For this purpose, a structure I CO_2 hydrate was chosen. The hydrate was grown from hexagonal ice Ih and the experiment was run until the conversion was complete. The reflection for the sI (321) crystal plane at circa 27.8° 2θ was used to illustrate the hydrate formation. Figure 6 shows the integrated intensity ratio of the (321) plane of CO_2 hydrate as a function of time for three experiments that were run under the same conditions. Each time the hydrate was grown at 1.16 MPa and 267 K. The hydrate formation was followed for 8.5 h for two experiments and for 7 h for the third experiment. After an experimental run-time of approximately 2 h, the data points show a wider distribution and larger error bars. This is significant for each of the three experimental runs and exclusively for CO_2 hydrate formation. The reason might be an inhomogeneous

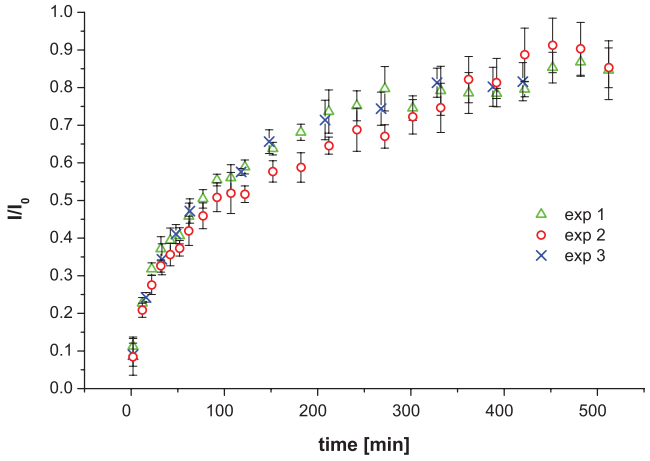

FIG. 6. (Color online) Intensity ratio I/I_0 as function of time during CO_2 hydrate formation. In order to show the reproducibility of the experimental setup, three experiments were conducted under the same conditions: 267 K and 1.16 MPa.

formation of structure I CO_2 hydrate crystals. Nevertheless, from Fig. 6, it becomes apparent that the data points of each run lie within the error bars of the other experiments proving the reproducibility of this experimental setup.

IV. SUMMARY

The pressure cell presented here allows the systematic analysis of reaction kinetics of simple and notably mixed gas hydrates depending on pressure, temperature, and feed gas composition. The unique feature of this setup is the continuous gas flow. Therefore, it can be assured that possible crystal structure transformations do not derive from changes in the feed gas phase (e.g., depletion of one guest species). The adjustment of pressure and temperature during the experiment is very convenient. According to requirements, the feed gas can be changed during the experiment as well. Because of fast data collection rates, the time resolution is very high. This is especially useful for investigations related to the start kinetics of hydrate formation or phase transformations. In addition to neutron and synchrotron XRD techniques, this setup is less expensive and can be used as a routine technique with a common X-ray diffractometer.

ACKNOWLEDGMENTS

The authors thank the staff of the GFZ workshops for invaluable technical help and for the construction of the pressure cell.

[1] J. A. Ripmeester, J. S. Tse, C. I. Ratcliffe, and B. M. Powell, Nature **325**, 135 (1987).
[2] E. D. Sloan and C. A. Koh, *Clathrate Hydrates of Natural Gases*, 3rd ed. (CRC, Boca Raton, 2007).
[3] R. W. Henning, A. J. Schultz, V. Thieu, and Y. Halpern, J. Phys. Chem. A **104**, 5066 (2000).
[4] X. Wang, A. J. Schultz, and Y. Halpern, J. Phys. Chem. A **106**, 7304 (2002).
[5] D. K. Staykova, W. F. Kuhs, A. N. Salamatin, and T. Hansen, J. Phys. Chem. B **107**, 10299 (2003).
[6] G. Genov, W. F. Kuhs, D. K. Staykova, E. Goreshnik, and A. N. Salamatin, Am. Mineral. **89**, 1228 (2004).
[7] C. A. Koh, J. L. Savidge, and C. C. Tang, J. Phys. Chem. **100**, 6412 (1996).
[8] C. C. Tang, C. A. Koh, A. A. Neild, R. J. Cernik, R. E. Motie, R. I. Nooney, and J. L. Savidge, J. Synchrotron Rad. **3**, 220 (1996).
[9] S. Takeya, T. Hondoh, and T. Uchida, Ann. N.Y. Acad. Sci. **912**, 973 (2000).
[10] S. Takeya, Y. Kamata, T. Uchida, J. Nagao, T. Ebinuma, H. Narita, A. Hori, and T. Hondoh, Can. J. Phys. **81**, 479 (2003).
[11] S. Takeya and J. A. Ripmeester, ChemPhysChem **11**, 70 (2010).
[12] S. Takeya and J. A. Ripmeester, Angew. Chem. Int. Ed. **47**, 1276 (2008).
[13] H. Lu, Y.-t. Seo, J.-w. Lee, I. Moudrakovski, J. A. Ripmeester, N. R. Chapman, R. B. Coffin, G. Gardner, and J. Pohlman, Nature **445**, 303 (2007).
[14] R. Sassen, S. T. Sweet, D. A. DeFreitas, J. A. Morelos, and A. V. Milkov, Org. Geochem. **32**, 999 (2001).
[15] R. L. Flemming, Can. J. Earth Sci. **44**, 1333 (2007).
[16] E. R. Wölfel, *Theorie und Praxis der Röntgenstrukturanalyse*, 3rd ed. (Vieweg, Braunschweig, 1987).